View metadata, citation and similar papers at core.ac.uk

brought to you by CORE

provided by Online Research Database In Technology

Technical University of Denmark

CTC-ask: a new algorithm for conversion of CT numbers to tissue parameters for Monte Carlo dose calculations applying DICOM RS knowledge

Cronholm, Rickard; Behrens, Claus F.

Published in:
Physics in Medicine and Biology

Link to article, DOI:
10.1088/0031-9155/56/22/N01

Publication date:
2011

Link back to DTU Orbit

Citation (APA):
Ottosson, R., & Behrens, C. F. (2011). CTC-ask: a new algorithm for conversion of CT numbers to tissue parameters for Monte Carlo dose calculations applying DICOM RS knowledge. Physics in Medicine and Biology, 56(22), N263-N274. DOI: 10.1088/0031-9155/56/22/N01

DTU Library
Technical Information Center of Denmark

General rights
Copyright and moral rights for the publications made accessible in the public portal are retained by the authors and/or other copyright owners and it is a condition of accessing publications that users recognise and abide by the legal requirements associated with these rights.

- Users may download and print one copy of any publication from the public portal for the purpose of private study or research.
- You may not further distribute the material or use it for any profit-making activity or commercial gain
- You may freely distribute the URL identifying the publication in the public portal

If you believe that this document breaches copyright please contact us providing details, and we will remove access to the work immediately and investigate your claim.

CTC–ask; a new algorithm for conversion of CT numbers to tissue parameters for Monte Carlo dose calculations applying DICOM RS knowledge

Rickard O Ottosson†‡¶,Claus F Behrens‡

† Risø National Laboratory, Technical University of Denmark, Roskilde, Denmark
‡ Copenhagen University Hospital Herlev, Department of Oncology (R), Division of Radiophysics (52AA), Herlev, Denmark

Abstract. One of the building blocks in Monte Carlo treatment planning is to convert patient CT data to Monte Carlo compatible phantoms, consisting of density and media matrices. The resulting dose distribution is highly influenced by the accuracy of the conversion. Two major contributing factors are precise conversion of CT number to density and proper differentiation between air and lung. Existing tools do not address this issue specifically. Moreover, their density conversion may depend on the number of media used.

Differentiation between air and lung is an important task in Monte Carlo Treatment Planning and misassignment may lead to local dose errors on the order of 10%.

A novel algorithm, CTC–ask, is presented in this study. It enables locally confined constraints for the media assignment and is independent of the number of media used for the conversion of CT number to density. Monte Carlo compatible phantoms were generated for two clinical cases using a CT–conversion scheme implemented in both CTC–ask and the DICOM–RT toolbox. Full Monte Carlo dose calculation was subsequently conducted and the resulting dose distributions were compared.

The DICOM–RT toolbox inaccurately assigned lung in 9.9% and 12.2% of the voxels located outside of the lungs for the two cases studied, respectively. This was completely avoided by CTC–ask.

CTC–ask is able to reduce anatomically irrational media assignment.

The CTC–ask source code can be made available upon request to the authors.

¶ To whom correspondence should be addressed (riolot01@heh.regionh.dk)

1. INTRODUCTION

One of the building blocks in Monte Carlo (MC) Treatment Planning is to convert CT numbers to an MC compatible phantom, consisting of a density– and a media matrix. A protocol for automatic conversion was suggested by du Plessis et al. [1998]. That protocol is, however, limited to the beam quality under consideration. The MC framework EGSnrc is distributed with a tool called *ctcreate* for this task [Kawrakow, 2000*a*; Walters et al., 2005]. The modus operandi for this tool is to read and sort CT files from a directory, prompt the user for a subset and resample the data on a user specified grid. The actual conversion is performed by division of the CT numbers into a user specified number of bins corresponding to different media. All voxels are assigned the medium of the bin its CT number belongs to. Each bin has a lower and upper value in terms of CT number and density. A linear relationship between CT number and density is established within each bin. Thus, the conversion to density might depend on the number of media. The DICOM–RT toolbox [Spezi et al., 2002] has its own version of this tool. The general workflow is similar and the conversion is performed using the same principles. The DICOM–RT toolbox allows the user to read the dose grid of a DICOM RD file and use it as the voxel grid. This ensures that the MC simulation will be on the same grid as dose calculated by the treatment planning system (TPS).

A stoichiometric calibration protocol establishing a direct relationship between medium composition and Hounsfield Units (HU) was suggested in Schneider et al. [1996] and Schneider et al. [2000]. Moreover they suggested that the media within the human body readily can be represented by a limited number of media. Vandersraeten et al. [2007] showed that the number of media can be chosen so that the error in dose, due to media assignment, is less than 1%. Implementation of the protocol suggested by Schneider et al. [2000] requires measurements as well as access to tissue–like materials with precise known chemical composition. Vandersraeten et al. [2007] highlights the importance of differentiating between media with dicreprancies in H– and Ca–content as this has a significant impact on the attenuation properties of a medium. They suggest tweaking of the CT–number boundaries between air and lung for each tumour site, depending on the presence of lung.

Using dual energy CT–scanners for determination of Z and ρ_{en} in a CT–image has been suggested in several studies (e.g. [Bazalova et al., 2008; Torikoshi et al., 2003, 2004]).

The existing tools and protocols for conversion of CT data to Monte Carlo parameters are limited to a global list of media, however not all media are likely to exist within a given organ or anatomical structure (hereafter referred to as structures). This might lead to anatomically incorrect medium assignment (e.g. a dense tumor might be assigned bone in some voxels or voxels outside of the body may be classified as lung) and ultimately resulting in an error in dose. Furthermore, this disables the use of media with an overlap in CT numbers, but distinct elemental compositions.

The purpose of this work was to develop, evaluate and test a new algorithm,

implemented in a MATLAB (Mathworks, Natlick, MA, USA) software solution, enabling global density conversion using partially linear HU–to–density–relationship while using structure specific media conversion ramps (i.e. the list of media eligible for assignment and their HU–ranges). Incorporation of the delineations contained in the DICOM RS file enables separation into local compartments based on anatomical regions.

2. MATERIALS AND METHODS

2.1. CT calibration

A CIRS Model 062 phantom (CIRS Tissue Simulation Technology, Norfolk, VA, USA) was used for determination of the CT–to–density conversion relationship. The epoxy–based phantom ($\rho = 1.01$ gcm^{-3}) accommodate a total of 17 inserts simultainously.

A total of eight different tissue equivalent materials (2 of each) and a water filled syringe were placed in the phantom (table 1). The phantom was placed in a Phillips Brilliance CT Big Bore (Phillips, Amsterdam, The Netherlands) such that the iso–center of the scanner was aligned with the center of the phantom. A clinical protocol with typical scanning parameters (120 kVp, 2–mm slice thickness) was selected and the scan was repeated 7 times. The CT images were read into MATLAB, using the dicomread function. Volumes of interest (VOI) were drawn around each insert for every scan. VOIs was also drawn outside of the phantom to obtain the CT number for air. The data was pooled to obtain the average CT number of each insert for the entire population of scans. The data set was fitted with linear equations for the soft tissue and bone materials, respectively:

$$\rho = 10^{-3} \times \begin{cases} 1.02H - 7.65 & : H \leq 55 \\ 0.58H + 467.79 & : H > 55 \end{cases} \tag{1}$$

The linear fits had R^2 greater than 0.99. The results are in agreement with the findings of Saw et al. [2005].

2.2. Generating a representative media set

Using tabulated composition (NIST [2011]; White et al. [1987]; Woodard and White [1986]) of a limited number of tissues and the measured relationship between density and HU it is possible to generate a representative set of media spanning the full range of HU values from air to cortical bone (Schneider et al. [2000]; Vandersraeten et al. [2007]). The scheme suggested by Schneider et al. [2000] was adopted, with one modification: The soft tissue range was divided in accordance with Vandersraeten et al. [2007], which assures dosimetric equivalence within 1%. In total, 19 media were generated (table 2). The first and second bins correspond to air and lung, respectively. The composition of the following bins were calculated according to equation 18 in Schneider et al. [2000]:

$$w_i = \frac{\rho_1 \left(H_2 - H\right)}{\left(\rho_1 H_2 - \rho_2 H_1\right) + \left(\rho_2 - \rho_1\right) H} \left(w_{1,i} - w_{2,i}\right) + w_{2,i} \tag{2}$$

with

Table 1. Physical densities and average CT number for the scanned materials. Uncertanties on CT numbers are given as 1 SD.

Material	Physical density gcm^{-3}	CT number
Air (20 C)	1.2041×10^{-3}	-998 (±3)
Water (syringe)	1.00	-7 (±14)
Lung (inhale)	0.20	-801 (±16)
Lung (exhale)	0.50	-494 (±16)
Breast (50/50)	0.99	-33 (±16)
Liver	1.07	55 (±17)
Muscle	1.06	51 (±15)
Adipose	0.96	-64 (±16)
Trabecular Bone 200 $mgcm^{-3}$	1.16	183 (±18)
Dense Bone 800 $mgcm^{-3}$	1.53	841 (±19)

$$H_1 \leq H \leq H_2,$$

where H is the average HU of the bin, ρ is the density of the media and w_i is the weight of element i. The media used for the interpolation were the same as in Schneider et al. [2000], i.e. adipose tissue 3 and adrenal gland (for bin #3), small intestine (wall) and connective tissue (for bin #4) and red/yellow marrow and cortical bone (for bins #5 through #19). The calculated compositions of the HU–bins are presented in table 2.

2.3. CTC–ask general work–flow

A MATLAB program, called CTC–ask (CT Create Applying DICOM RS Knowledge), was developed. CTC–ask uses the DICOM–RT toolbox to a large extent, either through function calls or by direct reuse of code segments. Figure 1 illustrates the general work–flow of the program. Firstly, the CT–matrix, CT– and dose–grid are read from the DICOM files. The bilinear CT–to–density relationship is calculated based on data points submitted by the user. An option to use a pre–saved relationship is also provided. The CT matrix is globally converted to a density matrix, with a grid corresponding to the dose–grid of the DICOM RD file. The structures in the DICOM RS file are sorted according to structure types (e.g. PTV, External, Avoidance etc.) and the user is queried for structure types to be considered. A list of the structures with the desired types is created and presented to the user along with an option to exclude specific structures. The external outline is a required structure and may not be excluded. A logical mask is generated for each selected structure, that is, a logical matrix of the same shape as the RD dose grid where true means that the voxel belongs to the specific structure. The user is requested to input names and upper CT number bounds for the possible media (hereafter referred to as a ramp–function) for each structure (the lower CT number bound of the first medium defaults to -1000, while the ith (i>1) uses the

Table 2. The binning–schemed used for this study. The HU range was divided into 19 bins, the first corresponding to the composition of air and the second to lung. The composition of the following bins were determined by (equation 2) where the media used for the interpolation were adipose tissue 3 and adrenal gland (for bin #3), small intestine (wall) and connective tissue (for bin #4) and red/yellow marrow and cortical bone (for bins #5 through #19).

		Elemental weight (w_i)											
Media	H	H	C	N	O	Na	Mg	P	S	Cl	Ar	K	Ca
HUrange1	-1000 – -950			75.7	23.2						1.3		
HUrange2	-950 – -100	10.3	10.5	3.1	74.9	0.2		0.2	0.3	0.3		0.2	
HUrange3	-100 – 15	11.2	50.8	1.2	36.4	0.1			0.1	0.1			
HUrange4	15 – 129	10.0	16.3	4.3	68.4	0.4			0.4	0.3			
HUrange5	129 – 200	9.7	44.7	2.5	35.9			2.3	0.2	0.1		0.1	4.5
HUrange6	200 – 300	9.1	41.4	2.7	36.8		0.1	3.2	0.2	0.1		0.1	6.3
HUrange7	300 – 400	8.5	37.8	2.9	37.9		0.1	4.1	0.2	0.1		0.1	8.2
HUrange8	400 – 500	8.0	34.5	3.1	38.8		0.1	5.0	0.2	0.1		0.1	10.0
HUrange9	500 – 600	7.5	31.6	3.2	39.7		0.1	5.8	0.2	0.1			11.6
HUrange10	600 – 700	7.1	28.9	3.4	40.4		0.1	6.6	0.2	0.1			13.1
HUrange11	700 – 800	6.7	26.4	3.5	41.2		0.2	7.2	0.3				14.4
HUrange12	800 – 900	6.3	24.2	3.7	41.8		0.2	7.8	0.3				15.7
HUrange13	900 – 1000	6.0	22.1	3.8	42.4		0.2	8.4	0.3				16.8
HUrange14	1000 – 1100	5.6	20.1	3.9	43.0		0.2	8.9	0.3				17.9
HUrange15	1100 – 1200	5.3	18.3	4.0	43.5		0.2	9.4	0.3				18.9
HUrange16	1200 – 1300	5.1	16.6	4.1	44.0		0.2	9.9	0.3				19.8
HUrange17	1300 – 1400	4.8	15.0	4.2	44.4		0.2	10.3	0.3				20.7
HUrange18	1400 – 1500	4.6	13.6	4.2	44.9		0.2	10.7	0.3				21.5
HUrange19	$>$ 1500	4.3	12.2	4.3	45.3		0.2	11.1	0.3				22.2

upper CT number bound of the $(i-1)$th medium). An option to use a pre–saved ramp–function is also implemented. As every voxel is allowed to belong to only one structure, the program iterates over the selected structures and generates a union–structure in the regions where structure–overlaps exist. In case of structure–overlaps the ramp–function of the overlapping structures are compared. If identical, the structure–union is assigned the ramp else the user is queried to specify one. The voxels belonging to the overlapping area are set to false for the overlapping parent–structures and to true for the generated structure–union. If any unions were found during the iteration a recursive call of the function is made. Each structure undergoes a separate conversion of CT number to media based on their ramp–function. A global media list is generated and each structure correlated to the global list. An option to set voxels outside of the external outline to air with zero density is implemented in order to emulate the procedure of treatment planning systems. The media matrices are subsequently added to a global media matrix. Finally, the data is written to an egs4phant file.

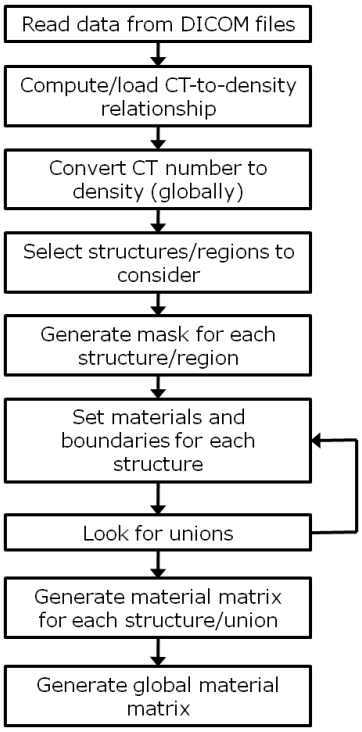

Figure 1. General work–flow of CTC–ask.

2.4. Patient cases

Two cases where one may expect improvements due to the specific considerations in CTC–ask were selected; a 15MV 3D–CRT pelvic case with substantial metal artifacts in the CT scan due to bilateral hip prostheses and a 6MV IMRT head an neck case including lung as well as air–filled cavities. Phantoms were generated based on the CT–data, using the 19 media conversion scheme as implemented in the DICOM–RT toolbox (hereafter referred to as unconstrained phantoms) as well as in CTC–ask (hereafter referred to as constrained phantoms). For the constrained pelvic phantom the bilateral hip prostheses were delineated, all voxels belonging to the delineated prostheses were set to titanium with a density of 4.54 gcm^{-3} and in the slices containing artifacts, all voxels inside the external outline not belonging to bone nor prostheses were set to ICRUTISSUE with a density of 1.00 gcm^{-3}. For the constrained head and neck phantom only voxels belonging to the lungs were allowed to be assign lung. Voxels inside the external outline, not belonging to any other specific structure, were allowed also to be assigned Cranium. As the mandible was outlined, voxels belonging to that structure were allowed also to be assign mandible as well. Compositions and densities of specific media were taken from Woodard and White [1986]. A second constrained phantom was generated for the head and neck case (hereafter referred to as constrained$_{air\ outside}$ phantom) where, in addition to previously mentioned considerations, voxels outside of the external outline all were assigned HUrange1 (corresponding to air) with a density of 1.2041×10^{-3} gcm^{-3}. The rationale behind this was to exclude the neck support tray

and the fixation mask from the MC–simulation.

2.5. Monte Carlo simulation

The MC simulations followed the procedure reported in Ottosson et al. [2010]. In short, EGSnrc and BEAMnrc [Kawrakow, 2000*a*,*b*; Rogers et al., 1995] were used to build and commission Monte Carlo models for each energy (6 and 15 MV) of a Varian 2300 iX linear accelerator (Varian Medical Systems, Palo Alto, CA, USA). A phase space file (PHSP) was scored just below the flattening filter for each of the energies. The PHSPs were scored by simulation of 2.5×10^6 histories with cut off energies of 521 keV (including rest mass) and 10 keV for electrons and photons, respectively. The beam modifiers and patient geometry were simulated in MCSIM [Jin et al., 2007; Ma et al., 2002] using the EGSnrc–generated PHSP as the source. A set of in–house MATLAB scripts were used to generate input files for MCSIM from the DICOM RP files. Thus, all parameters of the treatment plans were recreated in the simulations. The number of simulated histories were chosen so that the estimated statistical uncertainty[+] was $\approx 0.5\%$ for the voxels in the high dose regions. The selected number of histories resulted in estimated statistical uncertainties below 2%, 8% and 15% for voxels recieving 50%, 20% and 10% of the maximum dose, repsectively. All doses are reported as dose–to–medium.

3D–dose distributions were converted to DICOM RD files using CERR [Deasy et al., 2003] and subsequently imported to the TPS (Varian Eclipse 10.0) to generate DVHs.

3. RESULTS

The unconstrained phantoms were assigned HUrange2 (corresponding to lung) in 9.9% and 12.2% of voxels inside the external outline (excluding voxels belonging to lung structures) for the head and neck and the pelvic case, respectively. Moreover 15.1% of the larynx in the head and neck case was assigned lung in the unconstrained phantom. No voxels outside of the lung structures was assigned lung for the constrained phantoms (figure 2). The unconstrained phantoms also were assigned lung to voxels outside of the external outline. This was avoided for the constrained phantoms (figure 2).

Local differences in dose, for the clinically used treatment plans, were computed between constrained and unconstrained phantoms (the unconstrained phantoms were used as references). Histograms of the local differences for voxels inside the external outline and with statistical uncertainty on dose $\leq 2\%$ were produced (figure 3a–b). Gaussian–like distributions, with mean value close to zero, are noted when comparing constrained and unconstrained phantoms globally. For the head and neck case the

[+] The relative statistical uncertainty of the dose in a voxel is estimated by

$$\frac{\sigma D}{D} = \sqrt{\frac{n\sum e_i^2 - \left(\sum e_i\right)^2}{(n-1)\left(\sum e_i\right)^2}} \tag{3}$$

where e_i is the energy deposited in the voxel in the i^{th} energy deposition event and n is the total number of energy deposition events in the voxel.

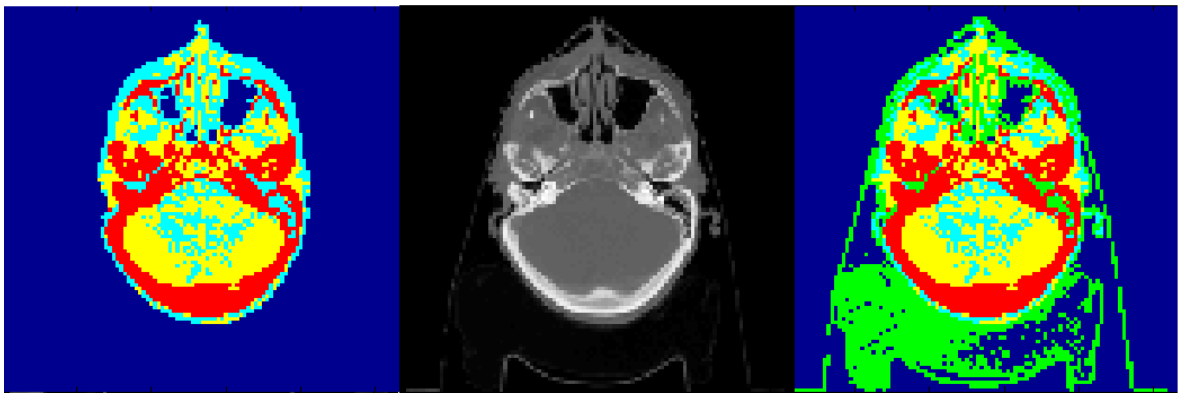

Figure 2. Transversal slice of the head and neck case showing media assignment for constrained$_{air\ outside}$ phantom, (left), HU–map (center) and media assignment for the unconstrained phantom (right). The colors correspond to air (dark blue), lung (green), soft tissue (cyan), connective tissue (yellow) and bone (red) (Note that all media corresponding to bone appear in red).

comparison between the constrained$_{air\ outside}$ and the unconstrained phantom deviate from this behaviour. Figure 3b show two things in particular for the constrained$_{air\ outside}$ phantom: (i) a low dose tail and (ii) a shift towards higher doses for the remaining distribution.

The user can make restrictions on which media CTC–ask is allowed to assign to voxels within a given structure. In order to investigate the influence of this on dose distribution in detail, the dose of voxels assigned specific media as well as voxels differing in terms of air and lung between the constrained and unconstrained phantoms were studied (figure 3c–d). When comparing dose in voxels assigned to lung in the unconstrained phantom while a different media in the constrained phantoms for the head and neck case two peaks are observed (figure 3c). The peaks are less distinct, but still existing, for the constrained$_{air\ outside}$ phantom.The dose for voxels assigned Cranium (figure 3d) in the constrained phantoms was lowered by $\approx$2% in average.

The Gaussian–like distribution around 0% for the pelvic case indicate that dose distributions generally agree. This is confirmed by the virtually indistinguishable DVHs of the external outline (figure 4a). For other structures, the differences are more noticable. A large underdosage is noted for the unconstrained PTV and almost the entire PTV volume receives 5 Gy less dose. On the other hand the bone and prostheses structures recieve higher doses in the unconstrained phantom. This is caused by the missasignment of media and density due to the metal artefacts. Differences in DVHs of the constrained and constrained$_{air\ outside}$ phantoms for the head and neck case are not as dramatic as the 5 Gy shift for the PTV of the pelvic case. Nevertheless it is evident that a larger volume recieves high doses for the constrained$_{air\ outside}$ (figure 4b). The effect is particularly noticable for deep–seated structures (e.g. PTV, larynx and spinal coord).

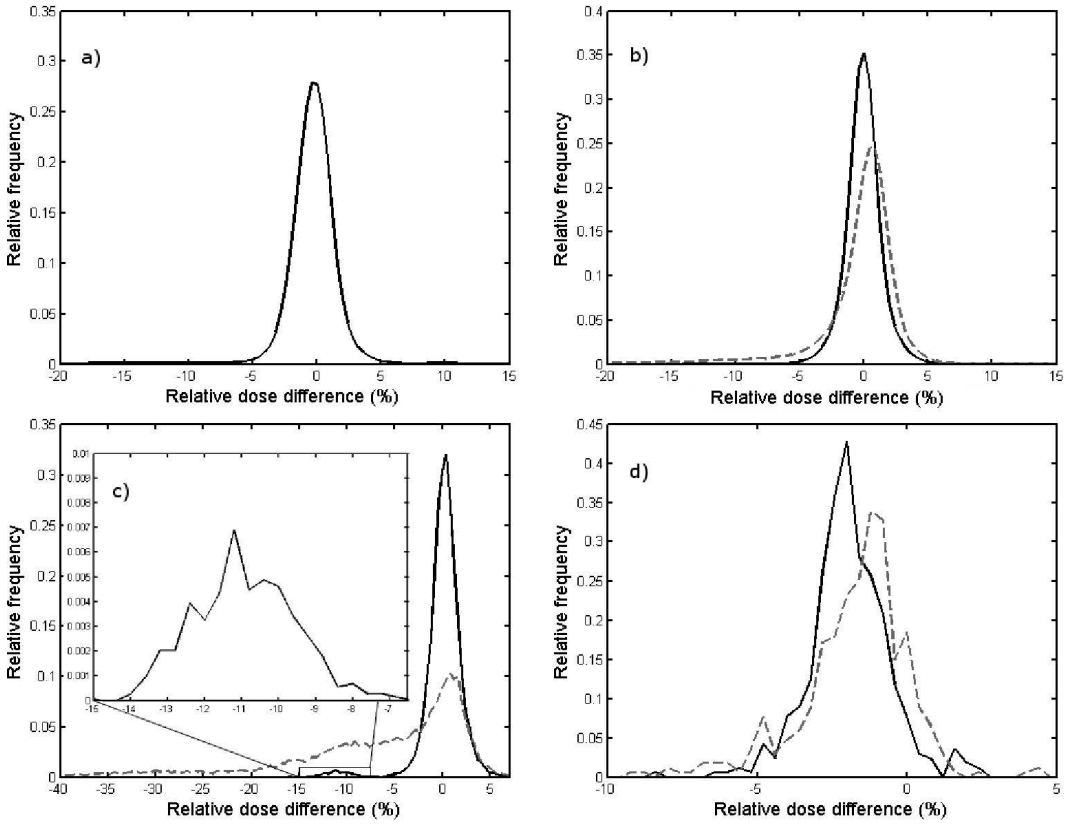

Figure 3. Histograms over local dose differences (calculated as ($\text{dose}_{constrained}$-$\text{dose}_{unconstrained}$)/$\text{dose}_{unconstrained}$ × 100) between constrained and unconstrained phantoms (solid) as well as $\text{constrained}_{air\ outside}$ and unconstrained phantoms (dashed) for the head and neck case. The histogram was plotted with a binwidth of 0.4% and normalized to the integral. Voxels outside the external outline or with uncertainty larger than 2% were ignored. **a)** Pelvic case. **b)** Head and neck case. **c)** For voxels in the head and neck case assigned HUrange2 (lung) in the unconstrained phantom and non–HUrange2 in the constrained phantoms. Two frequency peaks are noted for in the comparison with the constrained phantom (solid); around 0% and around -11%. The 0%–peak corresponds to voxels assigned HUrange3 (soft tissue) while the -11%–peak (also shown in the inserted figure) corresponds to voxels assinged HUrange1 (air) in the constrained phantoms, respectively. **d)** For voxels in the head and neck case assigned Cranium in the constrained phantoms (the corresponding voxels were assigned HUrange13 in the unconstrained phantom.)

4. DISCUSSION

The accuracy of MC dose calculation is strongly influenced by the conversion of CT–number to density and media. The most crucial contributor is arguably the density conversion. When assigning media to voxels, the most critical task is to differentiate between media with distinct mass attenuation properties. It was demonstrated that misassignment between air and lung can introduce a local error in dose in the order of 10% (figure 3c), which agrees with the findings of e.g. Verhaegen and Devic [2005].

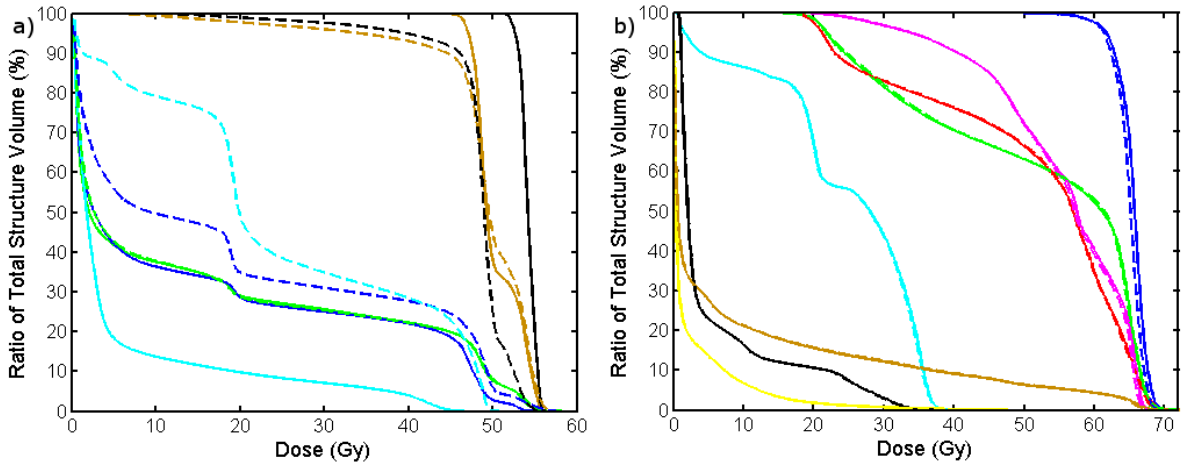

Figure 4. **a)** Cumulative dose volume histograms for the pelvic case using the constrained (solid) and unconstrained (dashed) phantoms. DVHs are plotted for the external outline (green), bones (blue), prostheses (cyan), PTV (brown) and the PTV excluding the rectum (black). **b)** Cumulative dose volume histograms for the head and neck case using the constrained$_{air\ outside}$ (solid) and constrained (dashed) phantoms. DVHs are plotted for the external outline (brown), PTV (blue), left parotid gland (red), right parotid gland (green), spinal cord (cyan), brainstem (black), larynx (magenta) and the lungs (yellow).

CTC–ask is run interactively and allows for manual manipulation at any point in time. This is useful in the case of CT–scans obtained with contrast enhancing agents and/or metal artifacts. For those cases the CT–number will not represent the actual density if not corrected for manually and dose calculation will be performed using the inaccurate densities and/or media. This can be solved by delineating the area containing the affected voxels and applying a filter that compensates for the shift in density (or CT–number) on those voxels. This was done for the constrained pelvic phantom, where voxels in slices containing metal artifacts were set to ICRUTISSUE with a density of 1.00 gcm^{-3} unless the voxels belonged to the delineated prostheses or bone structures. This heavily influenced the dose distribution of most structures (figure 4a). An alternative method of correcting for metal artifacts was presented by Bazalova et al. [2007] where the general idea is to apply a metal–filter and then by interpolating missing projections of the filtered sinograms. CTC–ask may be used in combination with the method suggested by Bazalova et al. [2007].

The inclusion of an "outside" structure, the inverse of the external outline, gives rise to the possibility of specifying which media that are allowed to be assigned outside of the patient. This is a unique feature for CTC–ask. Other existing tools allow any voxel to be assigned any of the media regardless of whether it is located within the body or not. Moreover, CTC–ask allows post–conversion manipulation of the density and/or media assignment for any structure. Hence, it is possible to set objects (couch, clothes, support structures etc) to air with zero density and thereby removing their influence on the dose calculation. This may influences the entire dose distribution. When setting

all voxels outside of the external outline to air for the head and neck case the build–up region is effectively shifted deeper into the patient. This is what causes the low dose tail (compared to the unconstrained phantom) for the constrained$_{air\ outside}$ phantom (figure 3b). Shifting the build–up region deeper also means that the beam will be less attenuated at a given distance beyond d_{max} and thus will give rise to a higher dose. This is the explanation for the shift towards higher doses in for the constrained$_{air\ outside}$ phantom (figure 3b and figure 4b). This effect will be somewhat compensated for distal voxels when using opposing beams while it will be further enhanced for central voxels. Assigning all of the voxels outside the external contour to air might not be accurate from a dosimetric point of view since the patient might be covered by a mask, be placed in a fixation and the treatment couch might be in the beam. In CTC–ask delineated support structures may, like any other delineated structure, be assigned the actual density and media compistion should it be known.

Vandersraeten et al. [2007] stress the importance of differentiating between air and lung (i.e. HUrange1 and HUrange2 in this study) and media with different Ca–content. Their suggested solution is to tune the CT–number boundary between air and lung depending on the tumor site and to include a number of media, with increasing Ca–content, representing bone of various densities. The CT–number of air and lung are however not likely to differ depending on tumor site. Another way to address the issue would be to exclude air and/or lung from areas where they are not likely to exist. This is what is done in CTC–ask. Moreover it is possible to tune the HUrange corresponding to a given media individually for each structure. Thus, a voxel with a HU of -940 might be assigned air, lung or gas depending on which structure it belongs to. In addition to the possibility of using a range of interpolated media representing tissues of various densities, CTC–ask allows for inclusion of tissue–specific media (and non–tissue media), and for confinement of the eligibility of those media to structures where they are likely to exist.

Media with distinct composition will likely differ in important dosimetrical properties (such as stopping power and mass energy absorption coefficients). This is illustrated by figure 3d, where the voxels assigned Cranium are shifted to a lower dose for the constrained phantoms due to lower mass stopping power of the composition corresponding to Cranium–media than that of HUrange13, which was the media assigned to the corresponding voxels in the unconstrained phantom.

Compton effect is the dominating effect for radiotherapy beams and the probability for Compton interaction is proportional to the electron density. Hydrogen has a higher electron density than elements with higher Z, therefore the attenuation properties of media will depend heavily on the hydrogen content. This is most outspoken when comparing air and lung as lung contain 10.3% hydrogen, whearas dry air does not contain any [Vandersraeten et al., 2007]. This is illustrated by (figure 3c) where two peaks are evident for the constrained phantom (solid line). For the voxels constituing the largest peak, around 0%, the voxels were assigned HUrange3 (soft tissue) whereas voxels in the peak around -11% (see insert in figure 3c) the voxels were assigned HUrange1

(air). The difference in hydrogen content is small (0.9%) when moving from HUrange2 to HUrange3 and thus no large effect on dose is expected for those voxels. The peaks are not as distinct for the constrained$_{air\ outside}$ phantom since the build–up region is shifted deeper into the patient in the constrained$_{air\ outside}$ phantom and a large fraction of the voxels are situated at shallow depths.

Erroneous assignment of media will lead to a local error in dose (figure 3c–d), which may or may not be partially compensated for, due to the differences in mass stopping power, if converting to dose–to–water (D_w). The mass attenuation of the improper media will however also perturb the beam, leading to an error in dose downstream or laterally. In addition, an increased backscatter (or lack thereof, depending on if moving from media with high H– or Ca– content to media with low, or vice versa) is noted at the boundary. Moreover, the local dose may be affected by media misassignment of neighboring voxels. None of those effects are compensated for when converting to D_w.

As CTC–ask utilize delineated structures in the DICOM data it is integral to ensure that the structures of consideration were properly delineated.

5. CONCLUSIONS

CTC–ask utilizes delineated structures in the DICOM data to set local conversion constraints for each structure and thus greatly reduces the probability of voxels being assigned anatomically irrational media. Furthermore, CTC–ask uses the CT–number to density–relationship without any linear interpolation within the range of media. Thus, the density matrix generated by CTC–ask will be independent of the number of media considered.

CTC–ask is run interactively and density and media matrices can be manually modified at any point. This gives rise to the possibility of applying filters to specific regions affected by contrast enhancing agents, metal artifacts etc. during the CT scan.

As CTC–ask relies on delineated structures in the DICOM set, it is integral to ensure that all structures are properly delineated as irrational media assignment otherwise may be introduced.

Acknowledgments

This project was granted by The Danish Cancer Society and supported by CIRRO - The Lundbeck Foundation Center for Interventional Research in Radiation Oncology and The Danish Council for Strategic Research. The hardware used for the MC calculations was donated by Toyota-Fonden, Denmark.

References

Bazalova M, Beaulieu L, Pefalsky S and Verhaegen F 2007 *Med Phys* **34**, 2119–2131.

Bazalova M, Carrier J F, Beaulieu L and Verhaegen F 2008 *Radiotherapy and Oncology* **86**, 93–98.

Deasy J O, Blanco A I and Clark V H 2003 *Med Phys* **30**, 979–985.

du Plessis F C, Willemse C A, Lötter M G and Goedhals L 1998 *Med Phys* **25**, 1195–1201.

Jin L, Wang L, Li J, Luo W, Feigenberg S J and Ma C M 2007 *Phys Med Biol* **52**, 3549–3561.

Kawrakow I 2000*a* *Med Phys* **27**(3), 485–498.

Kawrakow I 2000*b* *Med Phys* **27**(3), 499–513.

Ma C M, Li J S, Pawlicki T, Jiang S B, Deng J, Lee M C, Koumrian T, Luxton M and Brain S 2002 *Phys Med Biol* **47**, 1671–1689.

NIST 2011 *http://physics.nist.gov/cgi-bin/Star/compos.pl?ap* .

Ottosson R O, Karlsson A and Behrens C F 2010 *Phys Med Biol* **55**, 4521–4533.

Rogers D W O, Faddegon B A, Ding G X, Ma C M, We J and Mackie T R 1995 *Med Phys* **22**(5), 503–524.

Saw C B, Loper A, Komanduri K, Combine T, Huq S and Scicutella C 2005 *Med Dosim* **30**, 145–148.

Schneider U, Pedroni E and Lomax A 1996 *Phys Med Biol* **41**, 111–124.

Schneider W, Bortfeld T and Schlegel W 2000 *Phys Med Biol* **45**, 459–478.

Spezi E, Lewis D G and Smith C W 2002 *Phys Med Biol* **47**, 4223–4232.

Torikoshi M, Tsunoo T, Sasaki M, Endo M, Noda Y, Ohno Y, Kohno T, Hyodo K, Uesugi K and Yagi N 2003 *Phys Med Biol* **48**, 673–685.

Torikoshi T T M, Ohno Y, Endo M, Natsuhori M, Kakizaki T, Yamada N, Ito N, Yagi N and Uesugi K 2004 *Nuclear Science Symposium Conference Record, IEEE* **6**, 3764–3768.

Vandersraeten B, Chin P W, Fix M, Leal A, Mora G, Reynaert N, Seco J, Sokup M, Spezi E, Neve W D and Thierens H 2007 *Phys Med Biol* **52**, 539–562.

Verhaegen F and Devic S 2005 *Phys Med Biol* **50**, 937–946.

Walters B, Kawrakow I and Rogers D W O 2005 *http://www.irs.inms.nrc.ca/BEAM/user_manuals/pirs794/index.html* pp. 1–97.

White D R, Woodard H Q and Hammond S M 1987 *The Brittish Journal of Radiology* **60**, 907–913.

Woodard H Q and White D R 1986 *The Brittish Journal of Radiology* **59**, 1209–1219.